INNSPUB

Journal of Biodiversity and Environmental Sciences | JBES
ISSN: 2220-6663 (Print); 2222-3045 (Online)
Website: https://www.innspub.net
E-mail contact: info@innspub.net
Vol. 28, Issue: 1, p. 168-178, 2026

RESEARCH PAPER OPEN ACCESS

Using chitosan-based banana fruit peel waste in super nanocomposite to achieve batch equilibrium on dye adsorption

M. Priyanga[1], S. P. Mano Bala[1], V. Gomathi Priya[3], P. Bhuvaneswari[2], T. Shanmuga Vadivu[2], S. Viswanathan[3], G. Annadurai[1], R. Soranam[*1]

[1]*Sri Paramakalyani Centre of Excellence in Environmental Sciences, Manonmaniam Sundaranar University, Alwarkurichi, Tamil Nadu, India*

[2]*JP College of Arts and Science, Department of Chemistry, College Road, Agarakattu, Ayikudi, Tamil Nadu, India*

[3]*Post Graduate & Research Centre of Microbiology, Sri Paramakalyani College, Manonmaniam Sundaranar University, Alwarkurichi, India*

Key words: Chitosan, Banana fruit peel waste, Dye, Adsorption, Equilibrium studies

Received: 03 January, 2026 **Accepted:** 14 January, 2026 **Published:** 17 January, 2026

DOI: https://dx.doi.org/10.12692/jbes/28.1.168-178

ABSTRACT

Chitosan-based banana fruit peel synthesis by Sol-gel process on chitosan-based banana fruit peel waste in super nanocomposite is the focus of the current study. The waste products from banana fruit peels that were based on chitosan were examined for dye adsorption and described using FTIR spectroscopy, TGA, and SEM. A number of variables, including dosages, pH and temperature, were examined in relation to dye adsorption. According to the Freundlich and Langmuir isotherm, adsorption happens on a homogeneous surface through monolayer sorption in the absence of sorbed molecule interaction. The Langmuir equation outperformed the Freundlich equation in terms of fit. The maximum adsorption capacity was computed at various temperatures, pH levels, and dosages. Chitosan-based banana fruit peel has a higher adsorption capacity under the same experimental conditions, making it a potentially more beneficial material than inexpensive adsorbents for dye adsorption from aqueous solutions.

***Corresponding Author:** R. Soranam ✉ soranamr@gmail.com

INTRODUCTION

Dye is a common component of industrial effluent from industries such paints, leather, tanneries, paper, and textiles (Chandhru *et al.*, 2020; Ayele *et al.*, 2021; Jennifer Yhon *et al.*, 2023). Due to their carcinogenic, mutagenic, allergic, and toxic qualities, dyes can have negative impacts on human health and the environment even at concentrations below 1 mg/L (Hai *et al.*, 2007; Amel *et al.*, 2012; Seow *et al.* 2016; Dahri *et al.*, 2017). Rhodamine dye must be eliminated from wastewater prior to its release into natural water bodies because of these features. Due to their complex chemical structure, the majority of dyes are synthetic organic molecules that are very stable to heat, light, and oxidizing agents, making it difficult for them to degrade (Crini, 2006; Mahesh *et al.*, 2016; Jennifer Yhon *et al.*, 2023). For this kind of pollutant, different treatment techniques have been investigated, such as ion exchange (Wawrzkiewicz *et al.*, 2015; Suteu *et al.*, 2014), ozonation and oxidation processes (Bakheet *et al.*, 2013; Masoumbeigi *et al.*, 2015), chemical coagulation/flocculation (Rodrigues *et al.*, 2012; Teh*et al.*, 2016), and ultrafiltration (Mondal *et al.*, 2012; Buscio *et al.*, 2016; Jennifer Yhon *et al.*, 2023). However, these methods are linked to high energy consumption (Nguyen *et al.*, 2013; El-Sayed *et al.*, 2014), high costs (Katheresan *et al.*, 2018), and secondary pollution production (Hayder *et al.*, 2020). Consequently, alternative wastewater treatment has been the subject of research. According to Ahmaruzzaman *et al.* (2008), these techniques fall into three categories: biological, chemical, and physical. In large-scale wastewater treatment, continuous operations in fixed-bed columns are typically required to treat large volumes of contaminated water in shorter periods of time. However, several studies have demonstrated that various types of agricultural waste (biomass) can be competitive alternatives to activated carbon for batch processes (Akkaya and Guzel, 2014; De Oliveria Brito *et al.*, 2013; Lopez-Cabeza *et al.*, 2017; Jennifer Yhon *et al.*, 2023). Rhodamine dye can be effectively removed from banana peels, a cheap and accessible lignocellulosic agricultural waste, in both batch (Gallo-Cordova *et al.*, 2017; Sarici-Ozdemir, 2014; Akpome *et al.*, 2020) and continuous processes (Aurore *et al.*, 2009; Annadurai *et al.*, 2002; Jennifer Yhon *et al.*, 2023). This study examines the degree to which color adheres to banana fruit peel waste, a common agricultural waste, based on chitosan. With an emphasis on adsorption efficiency and batch equilibrium research, this work attempts to examine how operational factors affect the dye batch adsorption process employing chitosan-based banana fruit peel waste as the adsorbent. In order to determine the ideal local operating parameters within the study range, the investigation looks at adsorbent doses, temperature, and pH at three different levels. The adsorption behavior of chitosan-based banana fruit peel waste for the removal of the colors from textile wastewater was demonstrated by carefully fitting the experimental adsorption data with isotherm models.

MATERIALS AND METHODS

Chemicals, reagents, and media

The substances listed below were analytically graded. Merck provided the chitosan powder, sodium tripolyphosphate, acetic acid glacial (CH_3COOH) 100% GR (Merck), and double distilled water. Rhodamine dye was commercial product supplied by CDH Chemicals India.

Banana peel

We purchased the banana peel at the local market, Ambasamdrum, and Tirunelveli. The banana peels were cleaned with deionized water, freeze-dried, ground into a powder, and kept at 4°C for later use. When necessary, 20 g of dried and finely crushed banana peel was cooked in 100 ml of deionized water for 20 minutes at 60°C. The extract was then stored at 4°C for a week before being used in additional research after passing through a Millipore filter (0.45 m). They will be dried for 48 hours at 40 degrees Celsius before being ball-milled to a precise geometric size. The peels were pulverized, then labeled, packaged, and placed in an airtight container.

Preparation of chitosan nanoparticles

Chitosan high degree of protonation of amine functionalities and its capacity to form hydrogels in the presence of specific polyanions serve as the foundation for the ionic gelation method, which is used to create nanoparticles from the molecule. Nanoparticles are produced when chitosan is cross-linked with a substance like sodium tripolyphosphate (TPP) due to the opposing charges between the two molecules. The Ionic Gelation Process is used to create chitosan nanoparticles. The foundation of ionotropic gelation is polyelectrolytes' capacity to cross-link to create nanoparticles when opposing ions are present. The chitosan cation is produced by dissolving the chitosan polysaccharide in an acidic aqueous solution during the ionic gelation process. The polyanionic tripolyphosphate solution is then continuously spun as this solution is added. When opposing charges (positive and negative) combine and precipitate to form spherical particles, ionic gelation takes place in chitosan. Chitosan was diluted to 1% w and then dissolved in 2% (v/v) acetic acid to form a solution. Sodium tripolyphosphate (STPP) at 1% (w/v) was used as an ionic cross-linker. Chitosan nanoparticles were produced by sonicating 10 mL of chitosan solution with 1 mL of STPP for an hour at room temperature.

Synthesis of banana peel with chitosan nanocomposite

At room temperature, five grams of the produced chitosan nanoparticles were constantly agitated magnetically while dissolving in a solution of one part ethanol to one part water. The aforementioned reaction mixture was then mixed with 25 g of powdered banana peel. The suspension was vigorously churned for two to four hours prior to being submerged in a sonication bath for four hours. After centrifuging the finished product for 30 minutes to separate the Banana Peel with chitosan nanocomposite, it was dried in a hot air oven at 100°C.

Batch adsorption experiments

0.1 of the chitosan-Based Banana Fruit Peel nanocomposite were suspended in water for adsorption testing using a batch approach. In an Erlenmeyer flask, 100 mL of Rhodamine dye solution (20–100 mg/L) was mixed with chitosan-Based Banana Fruit Peel nanocomposite at varying pH values (5.3, 6.9, 7.6), temperatures (30°C, 45°C, and 60°C), and doses (1.0, 2.0, and 3.0g/L). The mixture was equilibrated for 24 hours at 60 rpm on a water shaker thermostat. The remaining concentrations of the adsorbate were ascertained by recording the absorbance of the supernatant at a maximum of 560 nm using a UV/Vis Spectrometer. A mass balance equation was used, to find the amount of dye adsorbed in each flask which was determined by the equation (1),

$$q_e = \frac{C_I - C_F}{m} \times v \quad (1)$$

Where, qe = Adsorbed amount (mg/g); C_I = initial concentration of (mg/L); C_F = Final concentration of (mg/L); V = Volume of adsorbate; m = Mass of adsorbent.

Table 1. Isotherms and their linear forms

Isotherm	Linear regression	Plot
Langmuir isotherm	$1 / q_e = (1 / q_m) + (1 / K_L q_m C_e)$	$1 / q_e .vs. 1 / C_e$
Freundlich isotherm	$Log(C_e) = Log(K_F) + 1 / nLog(C_e)$	$Log(q_e) .vs. Log(C_e)$

Langmuir and Freundlich isotherm

The sorption of dye into a porous adsorbent can be explained by the Langmuir and Freundlich isotherm , which has been successfully applied in numerous other actual sorption processes. The Langmuir theory's fundamental premise is that sorption occurs at particular locations inside the adsorbent. The isotherm equation was used to fit the data from the adsorption experiment used in this study to the sorbent doses, pH, and temperature. For systems with heterogeneous surface energies, the Freundlich isotherm is employed. The most practical way to display experimental data at various doses, pH levels, and temperatures is with a sorption isotherm. The

adsorption isotherms, as displayed in the Table 1, were investigated by computing the adsorption capacity under various parameter settings.

RESULTS AND DISCUSSION

Thermogravimetric (TGA)

Thermogravimetric analysis (TGA) is shown in Fig. 1. Strong thermal stability was indicated by the melting points (Tm), which were found to be much higher than the body typical temperature of 37°C. These compounds may act as plasticizers or pollutants, reducing the degree of crystallinity and complicating the organization of polymeric chains (Achack *et al.*, 2009; Aranaz *et al.*, 2010). Crystallinity is a crucial component that can have a big impact on the mechanical and physical properties of the banana peel nanocomposite with chitosan nanoparticle. Fig. 1 shows the derivative thermogravimetric analysis (TGA) curves for chitosan, banana peel, and the chitosan and banana peel biocomposite. It is believed that the weight loss of chitosan at 42°C is due to the chitosan losing surface moisture.

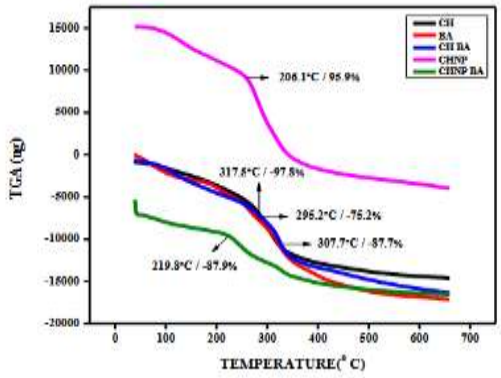

Fig. 1. TGA curves of the banana peel, chitosan with banana peel, chitosan nanoparticle, and chitosan nanoparticle with banana peel nanocomposite

Fourier transform infrared (FTIR)

The FTIR spectra with different concentrations of chitosan nanoparticles and banana peel nanocomposite are recorded in the 4000–400 cm−1 spectral range. The FTIR spectra are displayed in Fig. 2 the bands corresponding to pure chitosan and nanoparticles, respectively. Chitosan has a lot of functional groups, such as hydroxyl, carbonyl, carboxyl, amine, and amide, as can be seen from the spectra in Fig. 2. It is noteworthy that the addition of glycerol does not result in the acquisition of any additional bands in the chitosan spectra. The clear differences in the spectrum of pure chitosan and the composite material are depicted in the picture (Yoshida and Takemori, 1997). The O-H stretching vibration, which has a peak at 3418 cm−1, is expanded and moved to 3428 cm−1, increasing the intensity of the 2823 cm−1 band that corresponds to the C-H vibration. At 1645 cm−1, a new band that corresponds to the carboxyl group forms (Zheng, 2003). Fig. 2 displays the spectra of the composite membranes with different concentrations of chitosan nanoparticle and banana peel nanocomposite. According to the data, the strength of the amide peak at 1568 cm−1 has increased as the filler content has increased. The 2923 and 2924 bands, which are typical for the C-H, are increased as a result of the filler. The carboxyl group is represented by a new band that emerges at 1645 cm−1, which also intensifies the 1644 cm−1 band. This implies that the positively charged amine group in chitosan and the negatively charged carboxyl group in banana peels interact in some way, suggesting a carefully planned interaction between the filler and the matrix (Chen *et al.*, 2008).

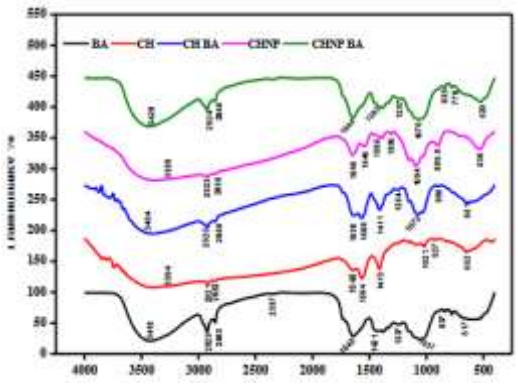

Fig. 2. FTIR curves of the banana peel, chitosan with banana peel, chitosan nanoparticle, and chitosan nanoparticle with banana peel nanocomposite

Scanning electron microscope (SEM)

Fig. 3 shows the SEM morphological structure of a banana peel nanocomposite containing chitosan nanoparticles. The particles measure 20–80 μm in length and 20–30 μm in width. The SEM's morphological structure with chitosan and banana peel powder concentrations is shown in Fig. 3.

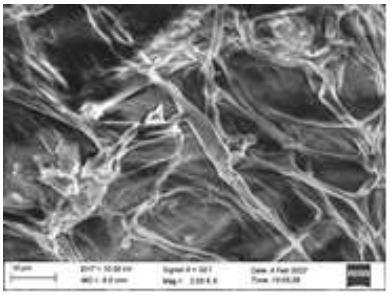

Banana

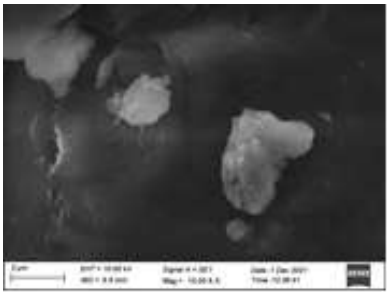

Chitosan

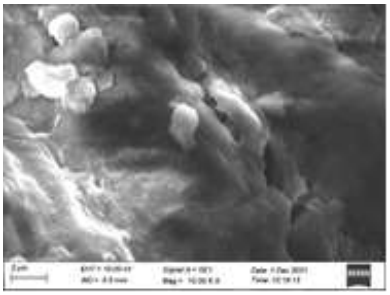

Banana chitosan

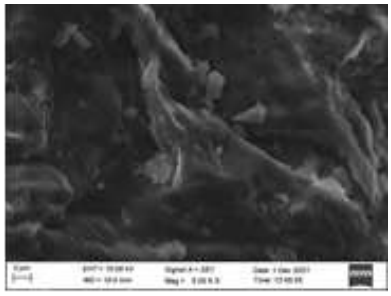

Chitosan nanoparticles

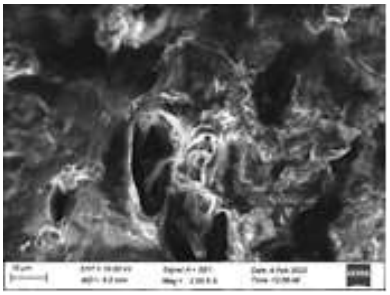

Banana chitosan nanoparticles

Fig. 3. SEM of the banana peel, chitosan with banana peel, chitosan nanoparticle, and chitosan nanoparticle with banana peel nanocomposite

SEM morphological analysis revealed that fillers for wound dressing were evenly distributed inside a chitosan matrix at a 5% weight concentration. There were several filler aggregates as a result of the filler concentration rising unevenly. The SEM images of the covering materials on banana fruit are shown in Fig. 3. Similar results were found by Kelly and Zweben (2000) using chitosan containing andiroba oil, demonstrating ellipsoidal and discontinuous structures associated with the formation of two phases in the matrix (lipid and polymer). Additionally, the number of oil droplets increased in tandem with the andiroba oil concentration. Feng *et al.* 2011 and Dutta *et al.*, 2009 reported similar results, demonstrating that plain chitosan membranes had dense, continuous, and uniform characteristics, while extracts containing chitosan from the first and third days of decoction displayed discontinuities and precipitates. These scientists point out that the results of the micrographs are caused by the presence of chemicals from the green banana peel extract, which structurally altered the chitosan matrix. Similar findings were made by Kelly (1985), who used chitosan and powdered green banana peels (0, 2, 5, and 10% by weight) to create micrographs that showed uniformly distributed filling within the chitosan matrix in the with 2% powder. Micrographs exhibiting very porous and heterogeneous structures with a succession of tiny white spots and a phase separation that grew thicker and more uniform as the extract concentration dropped were presented by Zheng *et al.* (2003) in accordance with this study. They were also researching banana peel extract and chitosan powder.

Langmuir isotherm studies

The conventional adsorption isotherms are used to show the relationship between the mass of adsorbate adsorbed per unit mass of the adsorbent and the equilibrium concentration of the adsorbate (Langmuir, 1918). Such isotherms are meant to give some insights into adsorption process and deduce certain constants and parameters to qualify adsorption mechanism (Venkateswarlu *et al.*, 2007; Altun and Pehlivan, 2007; Feng *et al.*, 2011; Mallampati and Valiyaveettil, 2012; Garg *et al.*, 2004; Mahmoodi *et al.*, 2005). Langmuir and Freundlich

isotherms describing the adsorption of dye on chitosan with banana peel nanocomposite. The Langmuir isotherm model is commonly used for sorption processes. It assumes that the adsorption occurs at specific homogeneous sites at the adsorbent surface and saturation is reached when the adsorbate fills up the sites and adsorption can chitosan with banana peel nanocomposite at different dosages, pH and temperature as shown in Fig.4-6.

$$q_e = \frac{KbC_e}{(1+bC_e)} \quad (2)$$

$$\frac{1}{q_e} = \frac{1}{K} + \frac{1}{KbC_e} \quad (3)$$

The various equations used for the isotherms (Eq 2-3). Batch mode adsorption studies were conducted and the effect of dosages, pH and temperature in the adsorption process were studies using the adsorbent, chitosan with banana peel nanocomposite. The optimum conditions for the dye removal were identified and presented in given table and graphs. The effect of dose of adsorbent on equilibrium time was examined by conducting batch mode experiments with 20 mg/L dye solution at the different pH at temperature with various doses of the adsorbent, namely 1.0 to 3.0g/L, respectively. The agitation speed and the size of the adsorbent were kept conducting experiments. The study of effect of dose of adsorbent is necessary and very useful to find out the optimum amount of sorbent required for the removal of dye. The effect of adsorbent studies is observed from 25.0 to 40 mg/g as shown in Fig . 4.

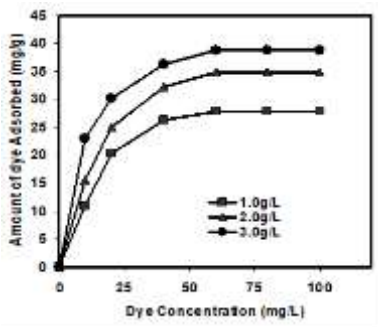

Fig. 4. Effect of specific dye uptake at different dosage chitosan-based banana fruit peel nanocomposite with rhodamine dye concentration

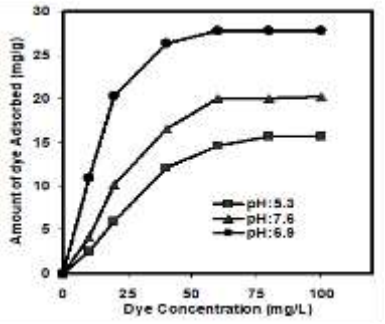

Fig. 5. Effect of specific dye uptake at different pH chitosan-based banana fruit peel nanocomposite with rhodamine dye concentration

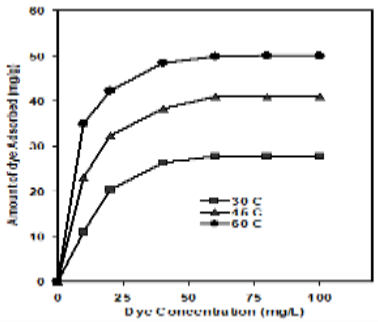

Fig. 6. Effect of specific dye uptake at different temperature chitosan-based banana fruit peel nanocomposite with rhodamine dye concentration

The amount of dye adsorbed increases with increase in sorbent dosage due to the availability of more surface-active sites for the adsorption of Rhodamine dye on the, chitosan with banana peel nanocomposite. Initially the rate of removal of dye is found to increase rapidly which slowed sown as the dose increased. The rate of adsorption is higher in the beginning as more free sites are available and uni molecular layers increase, From the observed results the dose of adsorbent at 3.0 g/L shows maximum removal of Rhodamine dye and after increase the dose of adsorbent there is no significant change. The pH of the solution is dominant parameter in controlling the adsorption process onto the adsorbent. Hence, the influence of pH in the removal of dye was examined initially and the optimum pH for the adsorption of the dye on, chitosan with banana peel nanocomposite was found effectively at pH 6.9 and a maximum of 28.0 mg/g of the dye was desorbed at this pH as shown in Fig. 5. From Fig. 6, it is obvious that the amount of the

dye adsorbed by the adsorbents decreases with increase in temperature. The maximum amount of Rhodamine dye by the adsorbents declines from 24.0 to 54.0 mg/g. When temperature was raised from 30 to 60°C, the retardation in the extent of adsorbate is due to the fact that at higher temperature the solubility of adsorbate increases and chemical potential decreases (Asfour *et al.*, 1968; Chiou *et al.*, 2004).

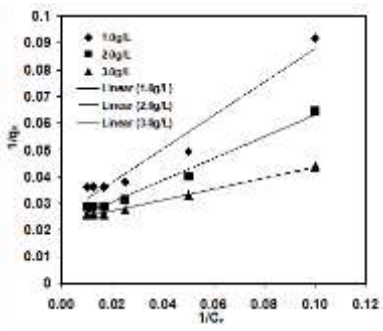

Fig. 7. Langmuir isotherm for the adsorption of rhodamine dye using chitosan-based banana fruit peel nanocomposite

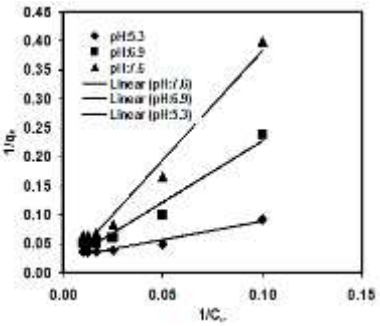

Fig. 8. Langmuir isotherm for the adsorption of rhodamine dye using chitosan-based banana fruit peel nanocomposite

As the temperature increases, the rate of diffusion of adsorbate molecules across the external boundary layer and interval pores of the adsorbent particles increases. Hence the change in the temperature will change the equilibrium capacity of the adsorbent for a particular adsorbate. A plot of ($1/q_e$ vs $1/C_e$) resulted in a linear graphical relation indicating the applicability of the above model as shown in (Fig. 7-9). The values are calculated from the slope and intercept of different straight line representing the different dosages, pH and temperature (b) energy of adsorption and (k) adsorption capacity and Q_0 is represented by (K).

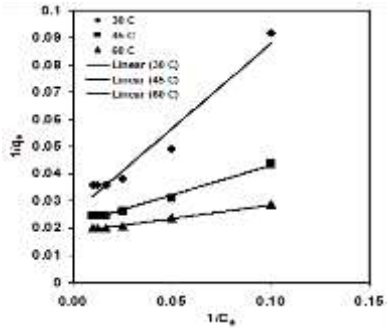

Fig. 9. Langmuir isotherm for the adsorption of rhodamine dye using chitosan-based banana fruit peel nanocomposite

Freundlich isotherm

The Freundlich isotherm is a model based on the adsorption of adsorbate onto heterogeneous surfaces. It is based on the assumption that the stronger binding sites are occupied first and the affinity for binding decreases with an increasing number of sites being occupied (Tang *et al.*, 2011; Negi *et al.*, 2012). The Freundlich isotherm is expressed by the following equation:

$$q_e = K_F C_e^{1/n} \quad (4)$$

$$\ln q_e = \ln K_F /(1/n) \ln C_e \quad (5)$$

K_F is the adsorption capacity of the adsorbent and it represents the amount of adsorbate adsorbed onto the adsorbent for a unit equilibrium concentration. The value of 1/n indicates that adsorption is favorable n<1, monolayer adsorption) and a value more than1 implies cooperative adsorption. The values of the constants can be determined from the intercept and slope of the linear plots of the experimental data of (ln q_e) versus (ln C_e) for the different dosages, pH and temperature as shown in (Fig, 10-12), following the equation below (Eq-4-5), Comparing the data in Table. 2, the Langmuir isotherm model showed the best fit with the highest R^2 value of 0.99 for most of the pollutants as compared to the Freundlich isotherm model. In addition, the values of 1/n are less than 1 for most of the pollutants for all sorbent, implying that a normal Langmuir isotherm is applicable.

Table 2. Langmuir and Freundlich isotherm constants at different adsorbent dosages, temperature, and pH. (Chitosan based banana fruit peel nanocomposite– Rhodamine dye)

Parameters		Langmuir Isotherm -model parameters (Type-I)	Freundlich Isotherm -model parameters
Dosage (g/ L)	1.0	K_L=0.040; q_m=39.21; R^2=0.9573	K_f=2.58 n=2.58; R^2=0.8361
	2.0	K_L=0.050; q_m=64.44; R^2=0.9814	K_f=2.90; n=0.88; R^2=0.8807
	3.0	K_L =0.11; q_m=43.47; R^2=0.9950	K_f=4.33; n=0.91; R^2=0.9132
Temperature (°C)	30	K_L =0.040; q_m=41.49; R^2=0.9573	K_f=1.38; n=0.388; R^2=0.8361
	45	K_L =0.098; q_m=40.0; R^2=0.9988	K_f=2.86; n=0.72; R^2=0.8856
	60	K_L =0.188; q_m=49.94; R^2=0.9678	K_f=3.24; n=0.37; R^2=0.8979
pH	5.3	K_L =0.002; q_m=53.47; R^2=0.9826	K_f=1.58; n=0.59; R^2=0.8361
	6.9	K_L =0.007; q_m=63.69; R^2=0.9656	K_f=0.12; n=0.40; R^2=0.8995
	7.6	K_L =0.040; q_m=39.21; R^2=0.9573	K_f=0.73; n=1.35; R^2=0.9324

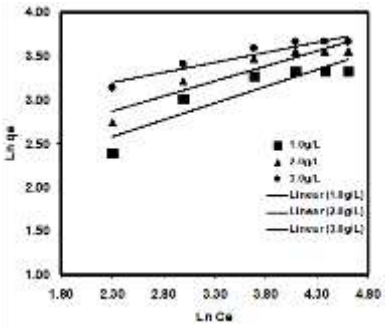

Fig. 10. Freundlich isotherm for the adsorption of rhodamine dye using chitosan-based banana fruit peel nanocomposite

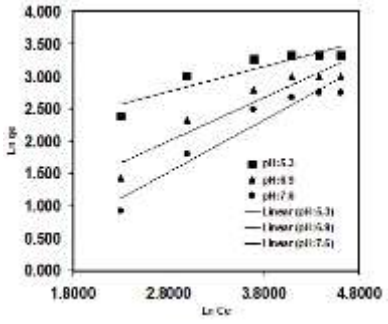

Fig. 11. Freundlich isotherm for the adsorption of rhodamine dye using chitosan-based banana fruit peel nanocomposite

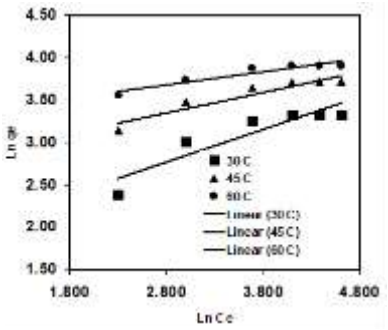

Fig. 12. Freundlich isotherm for the adsorption of rhodamine dye using chitosan-based banana fruit peel nanocomposite

The data also indicate a monolayer adsorption occurred at binding sites on the surface of the sorbent. The adsorption of rhodamine dye and neutral onto chitosan-based banana fruit peel nanocomposite follows the models of both isotherms as their R^2 values were comparable.

CONCLUSION

Based on the order rate mechanism, the Langmuir and Freundlich isotherm of sorption of rhodamine dye on a nanocomposite of banana fruit peels based on chitosan was investigated. The morphological and textural properties of the recently created chitosan-based banana fruit peel nanocomposite adsorbent were assessed by FT-IR, SEM, and TGA. Banana fruit peel has demonstrated a remarkable adsorption capacity for the removal of colors from textile effluents in chitosan-based products. Chitosan-based banana fruit peel morphology and thermal studies showed a high concentration of hydroxyl, amine, and carboxylic groups on the surface, which resulted in high interactions between the adsorbent and adsorbate, leading to high dye removal efficiency and adsorption capacity, according to the FTIR, SEM, and TGA studies. The wastewater solution has equal numbers of anions and cations, as indicated by the optimal adsorption at pH ~ 7. The adsorption capacity was negligible for adsorbent doses more than 3g/L, although increasing further with adsorbent dose. The equilibrium was attained after 24 hours of adsorption; however, because there were not enough adsorption sites, it took a bit longer for solution concentrations over 100 mg/L. The experimental adsorption data was well-fitted using a Langmuir isotherm model, indicating that the color removal technique employing banana fruit peel based on chitosan is a beneficial chemisorption method. This study demonstrates the high adsorption performance of banana peels made from renewable and inexpensive biowaste towards textile dyes. Furthermore, with additional acid and basic

treatments, approximately 95% of the banana fruit peel based on chitosan can be recovered and used again for additional color adsorption.

ACKNOWLEDGEMENTS

In order to complete this study M. Priyanga (Reg. 22214012052023) appreciates the Sri Paramakalyani Centre of Excellence in Environmental Science at Manonmaniam Sundaranar University in Alwarkurichi, India

REFERENCES

Achack M, Hafdini A, Ouazzani N, Sayadi S, Mandi L. 2009. Low cost biosorbent banana peel for the removal of phenolic compounds from olive mill wastewater: Kinetic and equilibrium studies. J. Hazard. Mater. **1661**, 117–125.

Ahmaruzzaman M. 2008.Adsorption of phenolic compounds on low-cost adsorbents: A review. Adv. Colloid. Interface Sci. **143**, 48–67.

Akkaya G, Guzel F. 2014. Application of some domestic wastes as new low-cost biosorbents for removal of methylene blue: Kinetic and equilibrium studies. Chem. Eng. Commun. **201**, 557–578.

Akpomie KG, Conradie J. 2020. Banana peel as a biosorbent for the decontamination of water pollutants. A Rev. Env. Chem. Lett. **18**, 1085–1112.

Altun T, Pehlivan E. 2007. Removal of copper (II) ions from aqueous solutions by walnut-, hazelnut- and almond-shells. CLEAN – Soil, Air, Water **35**, 601–606.

Amel K, Meniai A, Kerroum D. 2012. Isotherm and Kinetics Study of Biosorption of Cationic Dye onto Banana Peel. Energy Procedia **19,** 286–295.

Annadurai G, Juang RS, Lee, DJ. 2022. Use of cellulose-based wastes for adsorption of dyes from aqueous solutions. J. Hazard. Mater. **B92**, 263–274.

Aranaz I, Harris R, Heras A. 2010. Chitosan amphiphilic derivatives. Chemistry and applications. Current Organic Chemistry **14**, 308–330.

Asfour HM, Nasser MM, Fadali OA, El-Geundi MS. 1985. Colour removal from textile effluents using hardwood sawdust as an absorbent. J Chem Technol Biotechnology **35**, 28-35.

Aurore G, Parfait B, Fahrasmane L. 2009. Bananas, raw materials for making processed food products. Trends Food Sci. Technol. **20**, 78–91.

Ayele A, Getachew D, Kamaraj M, Suresh A. 2021. Phytoremediation of synthetic dyes: An effective and eco-friendly algal technology for the dye abatement. J. Chem. **20**, 9923643.

Bakheet B Yuan S, Li Z, Wang H, Zuo J, Komarneni S, Wang Y. 2013. Electro-peroxide treatment of orange II dye wastewater. Water Res. **47**, 6234–6243.

Blanco J. 2009. Review of feasible solar energy applications to water processes. Renewable& Sustainable Energy Reviews **13**(6–7), 1437–1445.

Buscio V, García-Jimenez M, Vilaseca M, Lopez-Grimau V, Crespi M, Gutiérrez-Bouzan C. 2016. Reuse of Textile Dyeing Effluents Treated with Coupled Nanofiltration and Electrochemical Processes. Materials **9**, 490.

Chandhru M, Rani SK, Vasimalai N. 2020. Reductive degradation of toxic six dyes in industrial wastewater using diaminobenzoic acid capped silver nanoparticles. J. Environ. Chem. Eng**. 8**, 104225.

Chen Y, Deng Q, Xiao J, Nie H, Wu L, Zhou W, Huang B. 2008. Controlled grafting from poly (vinylidene fluoride) microfiltration membranes via reverse atom transfer radical polymerization and antifouling properties. Polymer **48**, 7604-7613.

Chiou MS, Ho PY, Li HY. 2004. Adsorption of anionic dyes in acid solutions using chemically cross-linked chitosan beads. Dyes and Pigments **60**, 69-84.

Crini G. 2006. Non-conventional low-cost adsorbents for dye removal: A review. Bioresour. Technol. **97**, 1061–1085.

Dahri MK, Kooh MRR, Lim LB. 2013. Removal of methyl violet 2B from aqueous solution using Casuarina equisetifolia needle. Int. Sch. Res. **23**, 619819.

De Oliveira Brito SM, Andrade HMC, Soares LF, de Azevedo RP. 2013. Brazil nut shells as a new biosorbent to remove methylene blue and indigo carmine from aqueous solutions. J. Hazard. Mater. **174**, 84–92.

Dutta PK, Tripathi S, Mehrotra GK, Dutta J. 2009. Perspectives for chitosan based antimicrobial films in food applications. Food Chemistry **114**(4), 1173–1182.

El-Sayed HE, El-Sayed MM. 2014. Assessment of food processing and pharmaceutical industrial wastes as potential biosorbents: A review. Biomed. Res. Int. **20**, 146769.

Feng Y, Yang F, Wang Y, Ma L, Wu Y, Kerr PG, Yang L. 2011. Basic dye adsorption onto an agro-based waste material- Sesame hull (*Sesamum indicum* L.). Bioresources. Technol. **102**, 10280–10285.

Gallo-Cordova A, Silva-Gordillo M, Muuoz A, Arboleda-Fain X, Streitwieseer D. 2017. Comparison of the adsorption capacity of organic compounds present in produced water with commercially obtained walnut shell and residual biomass. J. Env. Chem. Eng. **5**, 4041–4050.

Garg VK, Kumar R, Gupta R. 2004. Removal of malachite green dye from aqueous solution by adsorption using agro-industry waste: a case study of *Prosopis cineraria*, Dyes Pigments **62**, 1–10.

Hai FI, Yamamoto K, Fukushi K. 2007. Hybrid Treatment Systems for Dye Wastewater. Crit. Rev. Environ. Sci. Technol. **37**, 315–377.

Hayde AA, Mohammed AK, Alaa HA. 2020. Removal of heavy metals from wastewater using agricultural byproducts. J. Water Suppl. Res. Technol. Aqua. **69**, 99–112.

Jennifer Yhon, Jeamilette Mendoza, Efren Osorio, María Paz Domínguez. 2023. Continuous Removal of Dyes from Wastewater Using Banana-Peel Bio adsorbent: A Low-Cost Alternative for Wastewater Treatment. Sustainability. **15**(13), 9870**.**

Katheresan V, Kansedo Sie Yon J. 2018. Efficiency of Various Recent Wastewater Dye Removal Methods: A Review. J. Environ. Chem. Eng. **6**, 4676–4697.

Kelley A, Zweben C. 2000. Comprehensive composite materials. Sci.dir, 1–6.

Kelly A. 1985. Composites in context: Compos Sci Technol. **23**(3), 171–99.

Langmuir I.1918. Adsorption of gases on plain surfaces of glass mica platinum. J Am Chem Soc. **40**, 1361-1403.

López-Cabeza R, Gamiz B, Cornejo J, Celis R. 2017. Behavior of the enantiomers of the herbicide 982 imazaquin in agricultural soils under different application regimes. Geoderma. **293**, 64–72.

Mahesh R, Gadekar M. 2016. Mansoor Ahammed. Coagulation/flocculation process for dye removal using water treatment residuals: Modelling through artificial neural networks. Des. Water Treat. **57**, 26392–26400.

Mahmoodi NM, Arami M, Yousefi Limaee N, Salman Tabrizi N. 2005. Decolorization and aromatic ring degradation kinetics of Direct Red 80 by UV oxidation in the presence of hydrogen peroxide utilizing TiO2 as a photocatalyst. Chem. Eng. J. **112**, 191–196.

Mallampati R, Valiyaveettil S. 2012. Application of tomato peel as an efficient adsorbent for water purification. Alternative biotechnology. RSC Adv. **2**, 9914–9920.

Masoumbeigi H, Rezaee A. 2002. Removal of Methylene Blue (MB) dye from synthetic wastewater using UV/H_2O_2 advanced oxidation process. Health Policy Sustain. Health **2**(1), 160–166.

Mondal S, Ouni, H, Dhahbi M, De S. 2012. Kinetic modeling for dye removal using polyelectrolyte enhanced ultrafiltration. J. Hazard. Mater. **22**, 381-389.

Negi R Satpathy G, Tyag YK, Gupta RK. 2012. Biosorption of heavy metals by utilizing onion and garlic wastes. Int. J. Environ. Pollut. **49**, 179–196.

Nguyen T, Ngo H, Guo W, Zhang J, Liang S, Yue Q, Li Q. 2013. Applicability of agricultural waste and by-products for adsorptive removal of heavy metals from wastewater. Biores. Technol. **148**, 574-585.

Rodrigues C, Madeirl L, Boaventura R. 2012. Treatment of textile dye wastewaters using ferrous sulphate in a chemical coagulation/flocculation process. Environ. Technol. **34**, 719–729.

Sarici-Ozdemir Ç. 2014. Removal of Methylene Blue by Activated Carbon Prepared from Waste in a Fixed-Bed Column. Partic. Sci. Technol. **32**, 311–318.

Seow TW, Lim CK, Nor MHM, Mubarak MFM, Lam CY, Yahya A, Ibrahim Z. 2016. Review on wastewater treatment technologies. Int. J. Appl. Environ. Sci. **11**, 111–126.

Suteu D, Bilba D, Coseri S. 2014. Macroporous polymeric ion exchangers as adsorbents for the removal of cationic dye basic blue 9 from aqueous solutions. J. Appl. Polym. Sci. **131**, 39620.

Tang PY, Wong CJ, Woo KK. 2011. Optimization of pectin extraction from peel of dragon fruit (*Hylocereus polyrhizus*). Asian J. Biol. Sci. **4**, 189–195.

Teht CY, Budiman PM, Shak PY, Wu TY. 2016. Recent Advancement of Coagulation–Flocculation and Its Application in Wastewater Treatment. Ind. Eng. Chem. Res. **55**, 4363–4389.

Venkateswarlu P, Ratnam MV, Rao DS, Rao MV. 2007. Removal of chromium from an aqueous solution using *Azadirachta indica* (neem) leaf powder as an adsorbent. Int. J. Phys. Sci. **2**, 188–195.

Wawrzkiewicz M, Hubicki Z, Kilislioglu A. 2015. Anion Exchange Resins as Effective Sorbents for Removal of Acid, Reactive, and Direct Dyes from Textile Wastewaters. Ion. Exchange **2**, 37–72.

Yoshida H, Takemori T. 1997. Adsorption of direct dye on cross-linked chitosan fibre: break through curve. Water Sci Technol. **35**, 29-37.

Zheng LY, Zhu JF. 2003. Study on antimicrobial activity of chitosan with different molecular weights. Carbohydrate Polymers **54**, 527–530.